Decaying magnetohydrodynamics: Effects of initial conditions

Abhik Basu*
Centre for Condensed Matter Theory, Department of Physics, Indian Institute of Science, Bangalore 560012, India
(Received 5 August 1999)

We study the effects of homogenous and isotropic initial conditions on decaying magnetohydrodynamics (MHD). We show that for an initial distribution of velocity and magnetic-field fluctuations, appropriately defined structure functions decay as a power law in time. We also show that for a suitable choice of initial cross correlations between velocity and magnetic fields even-order structure functions acquire anomalous scaling in time where as scaling exponents of the odd-order structure functions remain unchanged. We discuss our results in the context of fully developed MHD turbulence.

PACS number(s): 47.27.Gs, 05.45.−a, 47.65.+a

I. INTRODUCTION

In the absence of external forcing the fluid cannot maintain its steady state because of the continous dissipation of energy. The decay of kinetic energy in incompressible fluid turbulence has been explored in several studies (see, e.g., [1–3]). These studies, principally numerical, indicate that kinetic energy decays as $\sim(t-t_0)^{-\eta}$, where t_0 is the initial time, i.e., the time when the initial forcing is switched off. The value of η seems to depend on the initial state. Similarly, recent numerical studies of decaying magnetohydrodynamics (MHD) turbulence [3–6] also suggest that the total energy decays as a power of time. The phenomena of decaying MHD turbulence is observed in many different situations. Star-forming clouds are astrophysical examples [3].

Decay of MHD turbulence in a shell model

In Ref. [7] we described a shell model for MHD turbulence, which has all the conservation laws in the inviscid, unforced limit, has the right symmetries and reduces to the well-known Gledzer-Ohkitani-Yamada (GOY) shell model for fluid turbulence in absence of any magnetic field. In this paper we use our shell model to study decaying MHD turbulence. We begin by solving this set of equations with the external forces and by using the numerical method described there. We evolve the shell velocities v_n and magnetic fields b_n till we achieve the nonequilibrium, statistical steady state whose properties are described in Ref. [7]. Once we attain this state, say at a time $t=t_{ss}$, we use the last set of shell velocities and magnetic fields, i.e., $v_n(t_{ss})$ and $b_n(t_{ss})$, as the initial condition for our shell-model study of decaying turbulence in which we solve our shell-model equations but with all the forcing terms set equal to zero. We then use the resulting time series for v_n and b_n to determine the total energy $E(t)\equiv\Sigma_{\mathbf{k}}\langle|\mathbf{v}(\mathbf{k},t)|^2\rangle+\langle|\mathbf{b}(\mathbf{k},t)|^2\rangle$ and the total cross helicity $H^c(t)\equiv\langle|\mathbf{v}(\mathbf{k},t)\cdot\mathbf{b}(\mathbf{k},t)|\rangle$ where the origin of time is taken to be zero. We find that $E(t)\sim H^c(t)\sim t^{-p}$, with $p\simeq 1.2$; this is illustrated in the log-log plot of Fig. 1. As we have noted above, it is relevant for initial conditions that have the correct statistical properties of homogenous, isotropic MHD turbulence, which are well decribed by our shell model.

In a recent paper [8] the effects of random initial conditions on the decaying solutions of the unforced Navier-Stokes equation with hyperviscosity have been discussed: It has been shown that, for an initially Gaussian velocity distribution, equal-time two-point correlation functions like $\langle u(x,t)u(x,t)\rangle$ decay as $\sim t^{-1}$. It has also been shown that, for this particular choice of initial conditions, the theory remains finite (in a field-theoretic sense) just by renormalization of the two-point vertex functions. However, it is more relevant to explore the statistical properties of decaying fluid turbulence with ordinary viscosity. It is also important to find out how the introduction of magnetic fields influences this decay. In this paper we study decaying MHD with ordinary viscosity; we work with both the three-dimensional (3D) MHD equations and a *d*-dimensional generalization of the 1D MHD model introduced in Ref. [9]. We show that both these models give similar results. In particular, we show that, in both these models, appropriately defined structure functions decay with a power law in time; this is modulated by a scaling function whose form depends on the initial state. In Sec. II, we describe the equations we work with and the initial conditions we use. For most of the calculations in this Section, we choose initial correlations which are analytic in the low-wave-number limit. We choose ordinary viscosities for both velocity and magnetic fields. We calculate the *dynamic exponent z* and show that it is unaffected by the presence of the nonlinearities, i.e., it remains 2. We next show that if there is no initial cross correlation between velocity and magnetic fields, correlation functions defined at the same spatial point decay with power laws in time and, consequently, two-point structure functions also decay likewise. Also, multipoint correlation functions (and structure functions) exhibit similar behavior, with simple (and not anomalous) scaling in time. In other words, the exponents for high-order structure functions are simply related to those of two-point functions. Another interesting feature is that there is no change in the exponents with the introduction of the magnetic field (i.e., the exponents are the same for fluid and MHD turbulence); only the amplitudes of the correlation or structure functions change. In the Sec. III we show that in the presence of suitable cross correlations higher-order correlations (and consequently structure functions) decay more

*Also at Poorna Prajna Institute of Scientific Research, Bangalore, India.

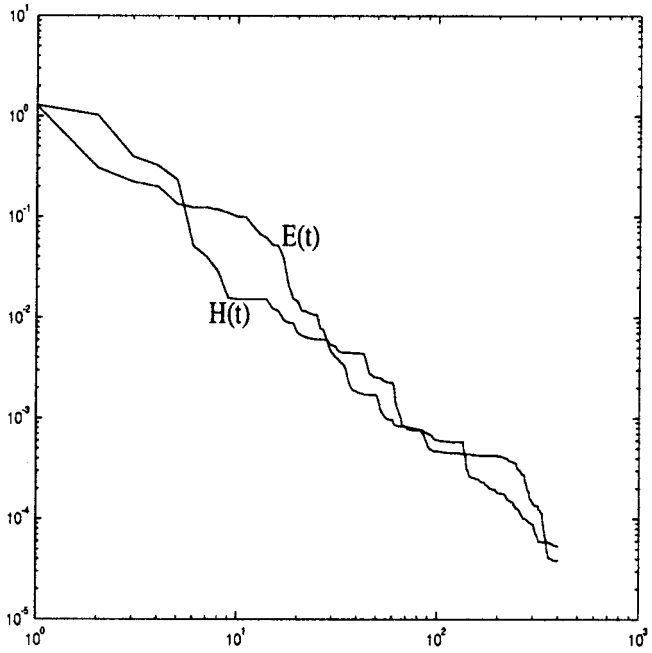

FIG. 1. A log-log plot of decay of total energy and cross helicity versus time.

slowly than when there is no cross correlation, i.e., they display anomalous scaling. In Sec. IV we extend and discuss our results in the context of the decay of fully developed MHD turbulence. In Sec. V we conclude and compare results obtained from both 3D MHD and our simplified model.

II. DECAYING MHD TURBULENCE: THE CASE OF ZERO INITIAL CROSS CORRELATION OF THE VELOCITY AND MAGNETIC FIELDS

A. Construction of a simplified model

The dynamical equations which govern the time evolutions of the velocity and magnetic fields in a magnetized fluid are given by the equations of magnetohydrodynamics, namely,

$$\frac{\partial \mathbf{y}}{\partial t}+(\mathbf{v}\cdot\boldsymbol{\nabla})\mathbf{v}=-\frac{\boldsymbol{\nabla} p}{\rho}+\frac{(\boldsymbol{\nabla}\times\mathbf{b})\times\mathbf{b}}{4\pi}+\nu\nabla^2\mathbf{v}+\mathbf{f_v}, \quad (1)$$

$$\frac{\partial \mathbf{b}}{\partial t}=\boldsymbol{\nabla}\times(\mathbf{v}\times\mathbf{b})+\mu\nabla^2\mathbf{b}+\mathbf{f}_b, \quad (2)$$

where $\mathbf{v}$ and $\mathbf{b}$ are the velocity and the magnetic fields, ν and μ are fluid and magnetic viscosities, p and ρ represent pressure and density, and $\mathbf{f_v}$ and $\mathbf{f_b}$ are external forces. We also impose the incompressibility condition $\boldsymbol{\nabla}\cdot\mathbf{v}=0$ and the divergence-free condition on the magnetic field $\boldsymbol{\nabla}\cdot\mathbf{b}=0$. In the absence of magnetic fields the MHD equations reduce to usual Navier-Stokes equation for fluid turbulence.

We now briefly present the ideas that go into the construction of the model, which has already been discussed in detail in [9]. Since this model is an extension of Burgers equation for fluid dynamics to MHD, it should have the following properties:

(i) Both the equations should be Galilean invariant.

(ii) The equations should be invariant under $t\rightarrow t$; $\mathbf{x}\rightarrow-\mathbf{x}$, $\mathbf{v}\rightarrow-\mathbf{v}$, and $\mathbf{b}\rightarrow\mathbf{b}$, i.e., the velocity field is odd parity and the magnetic field is even parity.

(iii) The fields are *irrotational* vector fields in d dimension (similar to Burgers velocity field).

(iv) The equations in the ideal limit, i.e., in the absence of any viscosity and any external forcing should conserve all the scalar conserved quantities of 3D MHD namely the total energy and the cross helicity. The third conserved quantity, i.e., the magnetic helicity is zero for irrotational fields.

The above considerations lead to the following model equations:

$$\frac{\partial \mathbf{y}}{\partial \mathbf{t}}+\frac{1}{2}\boldsymbol{\nabla} v^2+\frac{1}{2}\boldsymbol{\nabla} b^2=\nu\nabla^2\mathbf{v}+\mathbf{f_v}, \quad (3)$$

$$\frac{\partial \mathbf{b}}{\partial \mathbf{t}}+\boldsymbol{\nabla}(\mathbf{v}\cdot\mathbf{b})=\mu\nabla^2\mathbf{b}+\mathbf{f_b}, \quad (4)$$

whose relation to the 3D MHD equations is the same as the relation of the Burgers equation to the Navier-Stokes equation. Here $\mathbf{v}$ and $\mathbf{b}$ are the velocity and magnetic fields with magnitudes v and b, respectively. These fields are *irrotational*, i.e., $\boldsymbol{\nabla}\times\mathbf{v}=\mathbf{0}$ and $\boldsymbol{\nabla}\times\mathbf{b}=\mathbf{0}$. These equations together conserve the total energy $1/2\int(v^2+b^2)d^dx$ and cross helicity $\int\mathbf{v}\cdot\mathbf{b}\mathbf{d^d x}$.

B. Choice of initial conditions

We have $\langle u_i(k,t=0)\rangle=\langle b_i(k,t=0)\rangle=0$ by homogeneity and isotropy. We choose the initial correlations to have the simple analytic forms

$$\langle v_i(k,t=0)v_j(k',t=0)\rangle=D_{uu}k_ik_j\delta(k+k'), \quad (5)$$

$$\langle b_i(k,t=0)b_j(k',t=0)\rangle=D_{bb}k_ik_j\delta(k+k'), \quad (6)$$

and

$$\langle v_i(k,t=0)_ib_j(k',t=0)\rangle=D_{ij}(k)\,\delta(k+k'). \quad (7)$$

In k space the 3D MHD equations are

$$\partial_t v_i(\mathbf{p})+iM_{ijk}(\mathbf{p})\sum_q v_j(\mathbf{q})v_k(\mathbf{p}-\mathbf{q})$$

$$=iM_{ijl}(\mathbf{p})\sum_q b_j(\mathbf{q})b_l(\mathbf{p}-\mathbf{q})/4\pi\rho-\nu p^2v_i(\mathbf{p})+f_i(\mathbf{p}), \quad (8)$$

$$\partial_t b_i(\mathbf{p})=-\left(i\mathbf{p}\times\sum_q v(\mathbf{q})\times b(\mathbf{p}-\mathbf{q})\right)i$$

$$-\mu p^2b_i(\mathbf{p})+g_i(\mathbf{p}). \quad (9)$$

The quantities $M_{ijl}(\mathbf{k})=P_{ij}k_l+P_{il}k_j$ appear to include the incompressibility, $P_{ij}(k)=(\delta_{ij}-k_ik_j/k^2)$ is the transverse projection operator, and wave-vector arguments p,q,k indicate spatial Fourier transforms. The initial conditions we use for 3D MHD are

$$\langle u_i(k,t=0)u_j(k',t=0)\rangle=D_{uu}k^2P_{ij}(\mathbf{k})\,\delta(k+k'), \quad (10)$$

$$\langle b_i(k,t=0)b_j(k',t=0)\rangle = D_{bb}k^2 P_{ij}(\mathbf{k})\,\delta(k+k'), \quad (11)$$

$$\langle u_i(k,t=0)b_j(k',t=0)\rangle = D_{ij}(k)\,\delta(k+k'), \quad (12)$$

which ensure the divergence-free conditions, namely,

$$k_i\langle u_i(\mathbf{k})u_j(-\mathbf{k})\rangle = 0, \quad (13)$$

$$k_i\langle b_i(\mathbf{k})b_j(-\mathbf{k})\rangle = 0. \quad (14)$$

We discuss the structure of D_{ij} later. For the time being, we choose $D_{ij}=0$. These simple initial conditions, which are analytic in the $k\to 0$ limit, are enough to elucidate the issues raised in this section.

C. Calculation of effective correlation and structure functions within a one-loop perturbation theory: Temporal scaling

The formal solutions of the Eqs. (3) and (4) are given by

$$u_l(\mathbf{k},t) = e^{-\nu k^2 t}u_l(\mathbf{k},0) - \frac{i}{2}k_l\int_0^t dt'\int d^dp \times\exp[-\nu(t-t')k^2]\exp\{-\nu t'[p^2+(k-p)^2]\} \times[u_m(\mathbf{p},0)u_m(\mathbf{k}-\mathbf{p},0) + \exp\{-\mu t'[p^2+(k-p)^2]\} \times b_m(\mathbf{p},0)b_m(\mathbf{k}-\mathbf{p},0)] + \cdots, \quad (15)$$

$$b_l(\mathbf{k},t) = e^{-\mu k^2 t}b_l(\mathbf{k},0) - ik_l\int_0^t dt'\int d^dp \times\exp[-\mu(t-t')k^2]\exp\{-t'[\nu p^2+\mu(k-p)^2]\} \times[u_m(\mathbf{p},0)b_m(\mathbf{k}-\mathbf{p},0)] + \cdots, \quad (16)$$

where ellipsis refer to higher-order terms Similarly the formal solutions of the 3D MHD Eqs. (9) and (9) are given by

$$u_l(\mathbf{k},t) = e^{-\nu k^2 t}u_l(\mathbf{k},0) - \frac{i}{2}M_{ljs}\int_0^t dt'\int d^dp \times\exp[-\nu(t-t')k^2]\exp\{-\nu t'[p^2+(k-p)^2]\} \times[u_j(\mathbf{p},0)u_s(\mathbf{k}-\mathbf{p},0)$$

FIG. 2. One-loop diagrams contributing to the renormalization of ν.

$$-\exp\{-\mu t'[p^2+(k-p)^2]\}b_j(\mathbf{p},0)b_s(\mathbf{k}-\mathbf{p},0)] + \cdots, \quad (17)$$

$$b_l(\mathbf{k},t) = e^{-\mu k^2 t}b_l(\mathbf{k},0) - ik_m\int_0^t dt'\int d^dp \times\exp[-\mu(t-t')k^2]\exp\{-t'[\nu p^2+\mu(k-p)^2]\} \times[u_m(\mathbf{p},0)b_l(\mathbf{k}-\mathbf{p},0) - u_l(\mathbf{p},0)b_m(\mathbf{k}-\mathbf{p},0)] + \cdots, \quad (18)$$

where the ellipsis in refer to higher-order terms in the series. We use bare perturbation theory, i.e., after truncating the series at a particular order, all $\mathbf{v}$ and $\mathbf{b}$ are to be replaced by their bare values, i.e., by $G_0^u u(t=0)$ and $G_0^b b(t=0)$, respectively, where $G_0^u(\mathbf{k},t)=e^{-\nu k^2 t}$ and $G_0^b(\mathbf{k},t)=e^{-\mu k^2 t}$. This is similar to Ref. [10]. In the steady state of fluid or MHD turbulence, the *dynamic exponent* z is determined by the form of the correlations of the driving noise and dimensionality of the space. For example, when driven by noise correlations of the form k^{-3} (in 3D NS), one finds z (within a one-loop dynamic renormalization group calculation) to be 2/3 [11]. What is z when we study decaying MHD turbulence? We calculate this within a one-loop diagrammatic perturbation theory: In the bare theory (i.e., when the nonlinear terms are absent) $z=2$. If the one-loop corrections to the response functions (i.e., to the viscosities) have infrared divergence at zero external frequency, then $z<2$; otherwise $z=2$. The diagrams shown in Fig. 2 contribute at the one-loop level in renormalization of the fluid viscosity ν.

Similar diagrams renormalize μ. The effective one-loop fluid viscosity is given by

$$\frac{1}{\tilde{\nu}k^2} = \frac{1}{\nu k^2} + \frac{D_{uu}}{\nu k^2}\int d^3p\,\frac{p_l p_m \mathbf{k}\cdot(\mathbf{k}-\mathbf{p})}{2\nu\mathbf{k}\cdot\mathbf{p}}\left[\frac{1}{2\nu p^2 - 2\nu\mathbf{k}\cdot\mathbf{p}}\left(1-\frac{k^2}{\nu[p^2+(\mathbf{k}-\mathbf{p})^2]}\right) - \frac{1}{2\nu p^2}\left(1-\frac{k^2}{2\nu p^2}\right)\right] + \frac{D_{bb}}{\nu k^2}\int d^3p\,\frac{p_l p_m \mathbf{k}\cdot(\mathbf{k}-\mathbf{p})}{2\mu\mathbf{k}\cdot\mathbf{p}}\left[\frac{1}{2\mu p^2}\left(1-\frac{\nu k^2}{2\mu p^2}\right) - \frac{1}{2\mu p^2}\left(1-\frac{\nu k^2}{2\mu p^2}\right)\right]. \quad (19)$$

We see that, in the long-wavelength limit, one-loop corrections have no infrared divergence at $d=3$; in other words z remains 2. In the case of the 3D MHD equations, the forms of the integrals remain unchanged, only changes appear in the coefficients of the integrals where, in place of $p_l p_m$, appropriate projection operators are present. Thus again there is no diagrammatic correction to viscosities in the long-wavelength limit in 3D MHD. Hence the exponent z is unaffected by the nonlinear terms. Therefore, without any loss of generality, we can put $\nu=\mu=1$.

We now calculate the effective D_{uu} and D_{bb} for $d=3$ at the one-loop level. The diagrams shown in Fig. 3 contribute

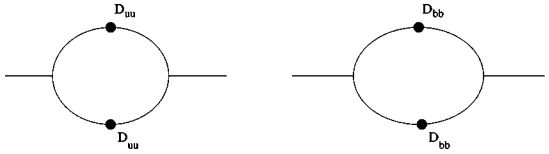

FIG. 3. One-loop diagrams contributing to the renormalization of D_{uu} and D_{bb}, respectively.

at the one-loop level to D_{uu}, These contributions are proportional to

$$k_i k_j (D_{uu}^2 + D_{bb}^2) \int d^3p \frac{p^2 p^2 (p^2 - k^2)^2}{k^4 p^8}$$

$$\sim k_i k_j (D_{uu}^2 + D_{bb}^2) \int^{\Lambda} d^3p, \tag{20}$$

which does not have any infrared divergence in *any dimension*. The one-loop diagram contributing to D_{bb} has the same form. For 3D MHD the forms of the one-loop integrals do not change; only the coefficients have appropriate factors of projection operators instead of $k_i k_j$. On purely dimensional grounds for $d=3$,

$$\langle u_i(\mathbf{x},t) u_j(\mathbf{x},t) \rangle \sim \int d^3k \langle u_i(\mathbf{k},t) u_j(-\mathbf{k},t) \rangle$$

$$\sim D_{uu} \int d^3k e^{-\nu k^2 t} e^{-\nu k^2 t} k_i k_j \sim D_{uu} t^{-5/2} \delta_{ij} \tag{21}$$

and

$$\langle b_i(\mathbf{x},t) b_j(\mathbf{x},t) \rangle \sim \int d^3k \langle b_i(\mathbf{k},t) b_j(-\mathbf{k},t) \rangle D_{bb}$$

$$\sim \int d^3k e^{-\nu k^2 t} e^{-\nu k^2 t} k_i k_j \sim D_{bb} t^{-5/2} \delta_{ij}. \tag{22}$$

Similar quantities obtained from 3D MHD also show the same exponents but with different amplitudes. [This is easy to understand: Calculation of the exponents through the one-loop method depends upon the power counting of the one-loop integrals which are same for both the 3D MHD equations and our simplified model as the projection operator P_{ij} that appears in the 3D MHD equations is dimensionless and the nonlinearities in both the equations do not renormalize due to the Galilean invariance of our simplified model and 3D MHD equations (which in turn keeps the power counting structure same). Amplitudes of course depend upon the specific models. Similarly, energy spectra obtained in the steady-state from different models which give same power counting in the one-loop integrals, when driven by stochastic forces with correlations having same scaling, have same scaling properties, see for e.g., Refs. [9,11].] Note that the temporal dependences can be scaled out of the momentum integrals easily as the lower and upper limits of the momentum integrals can be extended to 0 and ∞, respectively.

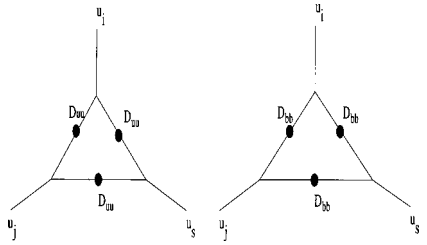

FIG. 4. One-loop diagrams contributing to $\langle u(\mathbf{k_1},t) u_j(\mathbf{k_2},t) u_s(\mathbf{k_3},t) \rangle$.

It is easy to see that all multipoint correlation functions also do not exhibit any infrared divergence in three dimensions: Consider, e.g., three-point functions. Even though $\langle u(\mathbf{k_1},t) u_j(\mathbf{k_2},t) u_s(\mathbf{k_3},t) \rangle = 0$ at $t=0$, it becomes nonzero at $t>0$ as can be easily seen at the one-loop level. $\langle u(\mathbf{k_1},t) u_j(\mathbf{k_2},t) u_s(\mathbf{k_3},t) \rangle$ has a tree-level contribution and next a one-loop contribution. The tree-level part being proportional to $\langle u_i(\mathbf{k_1},0) u_j(\mathbf{k_2},0) u_s(\mathbf{k_3},0) \rangle$ is zero because we have chosen a Gaussian distribution for the initial conditions. The one-loop diagrams are shown in Fig. 4.

The one-loop contribution is however nonzero. It has the form

$$\langle u(\mathbf{k_1},t) u_j(\mathbf{k_2},t) u_s(\mathbf{k_3},t) \rangle$$

$$\sim \exp[\nu(-k_1^2 - k_2^2 - (\mathbf{k_1}+\mathbf{k_2})^2)t] k_{1i} k_{2j}$$

$$\times (-k_{1s} - k_{2s}) D_{uuu}, \tag{23}$$

where D_{uuu} is the value of the one-loop integral in the limit $k_1, k_2 \to 0$, i.e.,

$$D_{uuu} \sim \int d^dq (D_{uu}^3 + D_{bb}^3), \tag{24}$$

which is infrared (IR) finite. We can interpret this one-loop result by saying that the nonlinearities in Eqs. (3) and (4) are absent but there are nonzero initial three-point correlations at $t=0$, i.e., the effective linear system behaves as if

$$\langle u_i(\mathbf{k_1},0) u_j(\mathbf{k_2},0) u_s(\mathbf{k_3},0) \rangle \equiv k_{1i} k_{2j} k_{3s} D_{uuu} \delta(\mathbf{k_1}+\mathbf{k_2}+\mathbf{k_3}), \tag{25}$$

$$\langle b_i(\mathbf{k_1},0) b_j(\mathbf{k_2},0) b_s(\mathbf{k_3},0) \rangle \equiv k_{1i} k_{2j} k_{3s} D_{bbb} \delta(\mathbf{k_1}+\mathbf{k_2}+\mathbf{k_3}). \tag{26}$$

Hence

$$\langle u_i(\mathbf{x_1},t)u_j(\mathbf{x_2},t)u_s(\mathbf{x_3},t)\rangle \equiv \int d^3k_1 d^3k_2 \exp[i\mathbf{k}_1\cdot(\mathbf{x_1}-\mathbf{x_2})+\mathbf{k_2}\cdot(\mathbf{x_1}-\mathbf{x_3})]\langle u_i(\mathbf{k_1},t)u_j(\mathbf{k_2},t)u_s(-\mathbf{k_1}-\mathbf{k_2},t)\rangle$$

$$= \int d^3k_1 d^3k_2 \exp[-k_1^2-k_2^2-(\mathbf{k_1}+\mathbf{k_2})^2]t \exp[i\mathbf{k_1}\cdot(\mathbf{x_1}-\mathbf{x_2})+\mathbf{k_2}\cdot(\mathbf{x_1}-\mathbf{x_3})]k_{1i}k_{2j}k_{3s}D_{uuu}$$

$$\sim t^{-9/2}A_{ijs}\left(\frac{\mathbf{x_1}-\mathbf{x_2}}{\sqrt{t}},\frac{\mathbf{x_1}-\mathbf{x_3}}{\sqrt{t}}\right). \tag{27}$$

The last step can be easily obtained by using the dimensionless variables $y_1=k_1^2t$, $y_2=k_2^2t$.

Next we consider the four-point functions: We concentrate on $\langle u_i(\mathbf{x_1},t)u_j(\mathbf{x_2},t)u_s(\mathbf{x_3},t)u_l(\mathbf{x_4},t)\rangle$; the diagrammatic representations up to the one-loop contributions are given in Fig. 5.

The one-loop integrals in the long-wavelength limit, are

$$D_{uuuu}\sim \int d^3q\left(\frac{D_{uu}^4}{\nu^4}+\frac{D_{bb}^4}{\mu^4}\right). \tag{28}$$

These one-loop contributions can be interpreted as in the previous case of three-point functions, i.e., as if there were initial four-point correlations in absence of the nonlinearities:

$$\langle u_i(\mathbf{k_1},0)u_j(\mathbf{k_2},0)u_s(\mathbf{k_3},0)u_l(\mathbf{k_4},0)\rangle \equiv D_{uuuu}k_{1i}k_{2j}k_{3s}k_{4l}\delta(\mathbf{k_1}+\mathbf{k_2}+\mathbf{k_3}+\mathbf{k_4}). \tag{29}$$

Similar results can be easily obtained for other four-point functions involving velocity and magnetic fields. Hence,

$$\langle u_i(\mathbf{x_1},t)u_j(\mathbf{x_2},t)u_s(\mathbf{x_3},t)u_l(\mathbf{x_4},t)\rangle \sim D_{uu}^2\int d^3k_1 d^3k_2 k_{1i}k_{1j}k_{2s}k_{2l}\exp[-2\nu(k_1^2+k_2^2)t]\exp[i\mathbf{k_1}\cdot(\mathbf{x_1}-\mathbf{x_2})+\mathbf{k_2}\cdot(\mathbf{x_3}-\mathbf{x_4})]$$

$$+D_{uuuu}\int d^3k_1 d^3k_2 d^3k_3 k_{1i}k_{2j}k_{3s}(-k_{1l}-k_{2l}-k_{3l})\exp[-\nu\{k_1^2+k^2+k_3^2$$

$$+(k_1^2+k_2^2+k_3^2)\}t]\exp[i\mathbf{k_1}\cdot(\mathbf{x_1}-\mathbf{x_2})+\mathbf{k_2}(\mathbf{x_2}-\mathbf{x_3})+\mathbf{k_3}(\mathbf{x_3}-\mathbf{x_4})]$$

$$\sim D_{uu}^2t^{-5}+D_{uuuu}t^{-13/2}. \tag{30}$$

In the infinite-Reynolds-number limit, i.e., in the limit $\nu,\mu\to 0$, $D_{uuuu}\to\infty$ and hence the second term in the last line of Eq. (30) dominates. As in the case for the three-point functions four-point functions, are of the form

$$\langle u_i(\mathbf{x_1},t)u_j(\mathbf{x_2},t)u_s(\mathbf{x_3},t)u_l(\mathbf{x_4},t)\rangle$$

$$\sim t^{-13/2}A_{ijsl}\left(\frac{\mathbf{x_1}-\mathbf{x_2}}{\sqrt{t}},\frac{\mathbf{x_2}-\mathbf{x_3}}{\sqrt{t}},\frac{\mathbf{x_3}-\mathbf{x_1}}{\sqrt{t}}\right). \tag{31}$$

Here A_{ijs} and A_{ijsl} are third and fourth rank tensors, respectively, and $\langle u_i(\mathbf{x},t)^4\rangle\sim t^{-13/2}$. To study decaying MHD, we extend the definition of equal-time structure functions as follows:

$$S_u^n(r,t)\equiv\langle|[u_i(\mathbf{x_1},t)-u_i(\mathbf{x_2},t)]|^n\rangle \tag{32}$$

and

$$S_b^n(r,t)\equiv\langle|[b_i(\mathbf{x_1},t)-b_i(\mathbf{x_2},t)]|^n\rangle, \tag{33}$$

where $r\equiv|\mathbf{x_1}-\mathbf{x_2}|$ and t denotes the time that has elapsed after the forcing terms are switched off. We now look at the general forms of these structure functions. Consider the three-point function first:

$$S_u^3(r,t)\equiv\langle|[u_i(\mathbf{x_1},t)-u_i(\mathbf{x_2},t)]|^3\rangle. \tag{34}$$

On expanding the expressions for, $S_u^3(r,t)$ we get the following kind of terms: (i) $\langle u_i(\mathbf{x_1},t)^3\rangle$ and (ii) $\langle u_i(\mathbf{x_1},t)^2u_i(\mathbf{x_2},t)\rangle$. The first one is given by

$$\langle u_i(\mathbf{x_1},t)^3\rangle = \int d^3k_1 d^3k_2 k_{1i}k_{2i}(-k_{1i}-k_{2i})$$

$$\times\exp[-\{k_1^2-k_2^2-(\mathbf{k_1}+\mathbf{k_2})^2\}t]D_{uuu}$$

$$\sim t^{-9/2}, \tag{35}$$

whereas the second term has the form

$$\langle u_i(\mathbf{x_1},t)^2u_i(\mathbf{x_2},t)\rangle = \int d^3k_1 d^3k_2 k_{1i}k_{2i}(-k_{1i}-k_{2i})$$

$$\times\exp[-\{k_1^2-k_2^2-(\mathbf{k_1}+\mathbf{k_2})^2\}t]$$

$$\times\exp[i\mathbf{k_1}\cdot(\mathbf{x_1}-\mathbf{x_2})]D_{uuu}$$

$$\sim t^{-9/2}\phi(r/\sqrt{t}), \tag{36}$$

with $r\equiv|\mathbf{x_1}-\mathbf{x_2}|$. Thus, it is easy to see that $S_u^3(r,t)$ has the structure

$$S_u^3(r,t)\equiv t^{-9/2}F_3^u(r/\sqrt{t}), \tag{37}$$

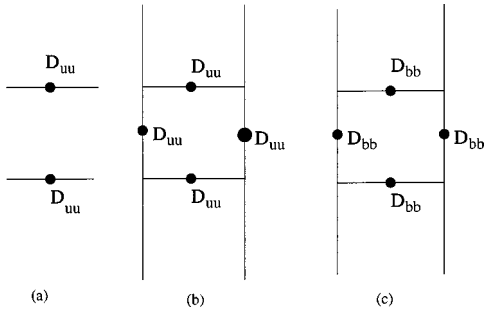

FIG. 5. Diagramatic contributions to $\langle u_i(\mathbf{k_1},t)u_j(\mathbf{k_2},t)u_s(\mathbf{k_3},t)u_l(\mathbf{k_4},t)\rangle$ up to one-loop level. (a) is the bare four-point function due to the initial two-point correlations, (b) and (c) are one-loop contributions.

with $F_3^u(r/\sqrt{t})$ is a function with dimensionless argument $r/\sqrt{t}$. We can easily extend our calculation above to see that

$$S_u^n(r,t)\sim t^{-z_n^u}F_n^u\left(\frac{r}{t^{1/2}}\right), \tag{38}$$

$$S_b^n(r,t)\sim t^{-z_n^b}F_n^b\left(\frac{r}{t^{1/2}}\right), \tag{39}$$

where F_n^u and F_n^b are functions with dimensionless argument $r/\sqrt{t}$. It is obvious that all these higher-order correlation functions do not exhibit any anomalous scaling in time; their temporal behaviors can be obtained by simple dimensional arguments from the behaviors of the two-point functions. It is easy to see that

$$S_u^n\sim t^{-(n-1)3/2-n/2}F_n^u\left(\frac{r}{t^{1/2}}\right), \tag{40}$$

$$S_b^n\sim t^{-(n-1)3/2-n/2}F_n^b\left(\frac{r}{t^{1/2}}\right), \tag{41}$$

i.e., $z_n^u=z_n^b=(n-1)3/2+n/2$, at the level of our one-loop approximation.

III. NONZERO INITIAL CROSS CORRELATIONS

A. Form of the initial cross correlations

What happens if we make D_{ij} nonzero? Let us first establish the form of D_{ij}: Recall that $\langle u_i(\mathbf{x_1},t)b_j(\mathbf{x_2},t)\rangle$ has odd parity (since **u** is a polar vector whereas **b** is an axial vector). Hence, it is purely imaginary and is an odd function of k. (From now on we will work only in three dimension.) Thus we choose

$$D_{ij}=iD_{ub}\epsilon_{ijp}k_pk^\alpha, \tag{42}$$

where ϵ_{ijp} is the totally antisymmetric tensor. This is the simplest analytic form with the desired structure. We consider the cases $\alpha=0$ and 2.

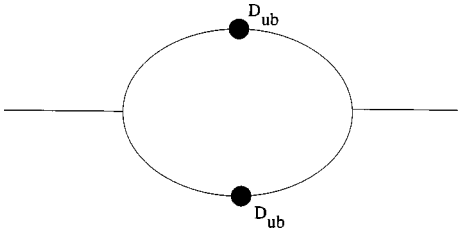

FIG. 6. One-loop diagram contributing to the renormalization of D_{uu} and D_{bb}, which arises when $D_{ub}\neq 0$ (see text).

B. The temporal decay of correlation and structure functions

It is easy to see that the value of z does not change if $D_{ub}\neq 0$ as no new diagram appears. However, an additional diagram (Fig. 6) contributes to the effective D_{uu} and D_{bb} if $D_{ub}\neq 0$.

This diagram yields the following contribution;

$$\frac{k_{1i}k_{2j}}{16k^4}D_{ub}^2\int\frac{d^3q}{(2\pi)^3}\frac{2\delta_{sn}q_sq_nq^\alpha}{q^2}, \tag{43}$$

where we have used the identity

$$\epsilon_{lms}\epsilon_{lmn}=(d-1)\delta_{sn}=2\delta_{sn}. \tag{44}$$

Naive power counting shows that this contribution is finite for $d=3$, hence D_{uu} and D_{bb} are not renormalized even if $D_{ub}\neq 0$, for both $\alpha=0$ and 2. The same conclusion holds for 3D MHD as the one-loop integral remains finite; only the coefficients change because of factors of $P_{ij}(k)$. It is quite interesting to note that for, $D_{ub}\neq 0$, there is a diagrammatic correction to D_{ub} (see Fig. 7).

The form of the correction is

$$\frac{k_{1i}k_{2j}}{16k^4}D_{uu}D_{ub}\int\frac{d^3q}{(2\pi)^3}\frac{q^\alpha\epsilon_{lms}q_sq_lq_m}{q^4}; \tag{45}$$

however, this correction vanishes for both $\alpha=0$ and 2 since the integrand is odd in q. Hence there is no renormalization of D_{ub} and two-point structure functions Eqs. (22) and (23) scale as $t^{-5/2}$ just as they do when $D_{ub}=0$.

C. Higher-order correlation and structure functions: Anomalous temporal scaling

We now consider the n-point correlation functions with $n>2$. None of the three-point functions have any infrared divergence. Hence they exhibit simple scaling, i.e., $\langle u_i(x,t)^3\rangle\sim t^{-9/2}$. Let us consider the four-point functions, namely,

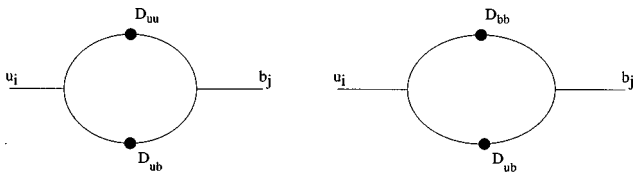

FIG. 7. One-loop diagrammatic correction to D_{ub}.

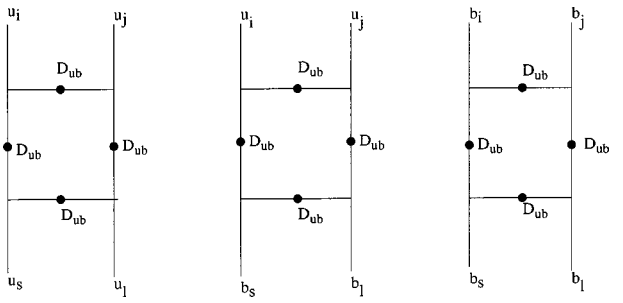

FIG. 8. Divergent one-loop contributions to $\langle u_i(\mathbf{x_1},t)u_j(\mathbf{x_2},t)u_s(\mathbf{x_3},t)u_l(\mathbf{x_4},t)\rangle$, $\langle u_i(\mathbf{x_1},t)u_j(\mathbf{x_2},t)b_s(\mathbf{x_3},t)b_l(\mathbf{x_4},t)\rangle$, $\langle b_i(\mathbf{x_1},t)b_j(\mathbf{x_2},t)b_s(\mathbf{x_3},t)b_l(\mathbf{x_4},t)\rangle$, respectively (see text).

$$\begin{aligned}&\langle u_i(\mathbf{x_1},t)u_j(\mathbf{x_2},t)u_s(\mathbf{x_3},t)u_l(\mathbf{x_4},t)\rangle,\\&\langle b_i(\mathbf{x_1},t)b_j(\mathbf{x_2},t)b_s(\mathbf{x_3},t)b_l(\mathbf{x_4},t)\rangle,\\&\langle u_i(\mathbf{x_1},t)u_j(\mathbf{x_2},t)b_s(\mathbf{x_3},t)b_l(\mathbf{x_4},t)\rangle,\\&\langle u_i(\mathbf{x_1},t)u_j(\mathbf{x_2},t)u_s(\mathbf{x_3},t)b_l(\mathbf{x_4},t)\rangle.\end{aligned}\tag{46}$$

At the one-loop level, all of them they will have finite parts (coming from initial auto correlations of velocity and magnetic fields). However, the first three of them will have new, *infrared-divergent*, one-loop contributions if $D_{ub}\neq 0$.

The analytic structure of the divergent one-loop integral is illustrated for one of these correlation functions in Fig. 8 whose contribution is

$$\begin{aligned}\langle u_i(\mathbf{k_1})u_j(\mathbf{k_2})u_s(\mathbf{k_3})u_l(\mathbf{k_4})\rangle \sim& \frac{k_{1i}k_{2j}k_{3s}k_{4l}}{k^8}\\&\times\int\frac{d^3p}{(2\pi)^3}\epsilon_{acm}\epsilon_{cdn}\epsilon_{def}\epsilon_{eat}\\&\times\frac{p_mp_np_fp_tp^\alpha}{p^8}.\end{aligned}\tag{47}$$

Isotropy yields

$$p_mp_np_fp_t=Ap^4[\delta_{mn}\delta_{ft}+\delta_{mf}\delta_{nt}+\delta_{mt}\delta_{fn}],\tag{48}$$

so summing over (m,n) and (f,t) separately we obtain

$$A=\frac{1}{d^2+2d}=1/15\tag{49}$$

for $d=3$. Hence naive power counting for the integral in Eq. (47) yields, for $\alpha=0$,

$$\sim\frac{k_{1i}k_{2j}k_{3s}k_{4l}}{15k^8}D_{ub}^4\int\frac{d^3pp^4}{p^8}\sim k_{1i}k_{2j}k_{3s}k_{4l}\Lambda^{-1},\tag{50}$$

where Λ is a momentum scale arising from the lower limit of the integral. Hence it is linearly infrared (IR) divergent for $\alpha=0$. For $\alpha=2$ there is no IR divergence as is the case with $D_{ub}=0$. We analyze the case $\alpha=0$ in detail: There is a disconnected diagram also that contributes to $\langle u_i(\mathbf{x_1},t)u_j(\mathbf{x_2},t)u_s(\mathbf{x_3},t)u_l(\mathbf{x_4},t)\rangle$, which yields

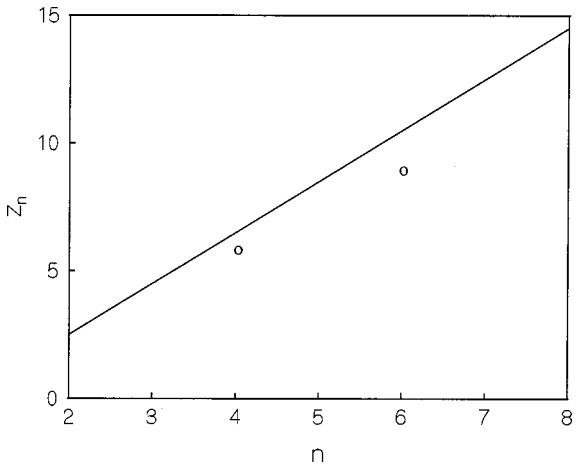

FIG. 9. A plot showing the dependence of z_n over n; the line gives the exponents for the odd order structure functions for all values of D_{ub} and for the even order structure functions when $D_{ub}=0$; we also show z_4 and z_6 in this plot (circles) when $D_{ub}\neq 0$ (for $\alpha=0$).

$$D_{uuuu}\sim D_{uu}^2.\tag{51}$$

This is finite in the $k\to 0$ limit, so the contribution from the connected part will dominate in the $k\to 0$ limit. If we define the effective four-point correlation to be $\propto D_{uuuu}\sim D^0_{uuuu}k^{-1}$ [with the choice $k=\sqrt{k_1^2+k_2^2+k_3^2+k_4^2}$), where D^0_{uuuu} is just a constant] then

$$\begin{aligned}&\langle u_i(\mathbf{k_1},0)u_j(\mathbf{k_2},0)u_s(\mathbf{k_3},0)u_l(\mathbf{k_4})\rangle\\&\quad\sim k_{1i},k_{2j}k_{3s}k_{4l}k^{-1}D^0_{uuuu}\delta(\mathbf{k_1}+\mathbf{k_2}+\mathbf{k_3}+\mathbf{k_4}).\end{aligned}\tag{52}$$

Hence one obtains

$$\begin{aligned}\langle u_i(\mathbf{x},t)^4\rangle\sim&\int d^3q_1d^3q_2d^3q_3\exp[-k_1^2-k_2^2-k_3^2\\&-(k_1+k_2+k_3)^2]t\times k_{1i}k_{2i}k_{3i}\\&\times(k_{1i}+k_{2i}+k_{3i})D^0_{uuuu}k^{-1}\\\sim&t^{-3d/2-2}t^{-1/2}\sim t^{-1/2}\langle u_i(\mathbf{x},t)^4\rangle|_{D_{ub}=0}.\end{aligned}\tag{53}$$

Similarly $\langle b_i(\mathbf{x},t)^4\rangle\sim t^{-1/2}\langle u_i(\mathbf{x},t)^4\rangle|_{D_{ub}=0}$, $\langle u_i(\mathbf{x},t)^2b_i(\mathbf{x},t)^2\rangle\sim t^{-1/2}\langle u_i(\mathbf{x},t)^2b_i(\mathbf{x},t)^2\rangle|_{D_{ub}=0}$. The other four-point functions are (dimensionally) linearly divergent at the one-loop level; however, the one-loop integral vanishes because the integrand is odd in p. Hence they will scale as $t^{-13/2}$. It is now obvious that

$$\begin{aligned}&\langle[u_i(\mathbf{x_1},t)-u_i(\mathbf{x_2},t)]^4\rangle\\&\quad\sim t^{-1/2}t^{-13/4}A_u\left(\frac{\mathbf{x_1}-\mathbf{x_2}}{t^{1/2}}\right)\\&\quad\sim t^{-1/2}\langle[u_i(\mathbf{x_1},t)-u_i(\mathbf{x_2},t)]^4\rangle|_{D_{ub}=0},\end{aligned}\tag{54}$$

$$\langle [b_i(\mathbf{x_1},t)-b_i(\mathbf{x_2},t)]^4\rangle \sim t^{-1/2}t^{-13/4}A_b\left(\frac{\mathbf{x_1}-\mathbf{x_2}}{t^{1/2}}\right) \sim t^{-1/2}\langle [u_i(\mathbf{x_1},t)-u_i(\mathbf{x_2},t)]^4\rangle|_{D_{ub}=0}. \quad (55)$$

Hence we see that these structure functions exhibit anomalous dynamical scaling if $D_{ub}\neq 0$. Similarly, it follows that the even-order exponents are

$$z^u_{2n}=z^b_{2n}=\frac{3}{2}(2n-1)+n-z^{\rm ano}_{2n},\ \ n\geqslant 2, \quad (56)$$

where $z^{\rm ano}_{2n}=(2n-3)/2$ is the *anomalous* part of the exponent z_{2n}. By contrast the odd order exponents

$$z^u_n=z^b_n=(n-1)3/2+n/2,\ \text{for any odd}\ n, \quad (57)$$

do not have an anomalous part. In Fig. 9 we present plots of z_n versus n for both even and odd n.

IV. EFFECTS OF INITIAL CONDITIONS WITH SINGULAR AMPLITUDES FOR THE VARIANCE

In this section we choose initial conditions of the following form:

$$\langle u_i(\mathbf{k},0)u_j(\mathbf{k}',0)\rangle = D_{uu}\frac{k_ik_j}{k^{s+2}}\,\delta(\mathbf{k}+\mathbf{k}'), \quad (58)$$

$$\langle b_i(\mathbf{k},0)b_j(\mathbf{k}',0)\rangle = D_{bb}\frac{k_ik_j}{k^{s+2}}\,\delta(\mathbf{k}+\mathbf{k}'), \quad (59)$$

and

$$\langle u_i(\mathbf{k},0)b_j(\mathbf{k}',0)\rangle = iD_{ub}\epsilon_{ijp}\frac{k_p}{k^{y+1}}\,\delta(\mathbf{k}+\mathbf{k}'). \quad (60)$$

We choose $s\geqslant y$. If $y>s$ then one-loop effective D_{uu} and D_{bb} will scale as k^{-y}. The effective fluid viscosity $\tilde{\nu}$, and two-point correlations $\tilde{D}_{uu}$ and $\tilde{D}_{uu}$ are given by

$$\frac{1}{\tilde{\nu}k^2}=\frac{1}{\nu k^2}+\frac{1}{\nu k^2}\int\frac{d^3p\,p^{-s}p_ip_jD_{uu}}{\nu[p^2+k^2-(k-p)^2]}\left[\frac{1}{\nu[p^2+(k-p)^2-k^2]}\left(1-\frac{k^2}{p^2+(k-p)^2}\right)\right]-\frac{1}{2\nu p^2}\left(1-\frac{k^2}{p^2}\right)\mathbf{k}\cdot(\mathbf{k}-\mathbf{p}) + \frac{1}{\nu k^2}\int\frac{d^3p\,p^{-s}p_ip_jD_{bb}}{\mu[p^2+k^2-(k-p)^2]}\left[\frac{1}{\mu[p^2+(k-p)^2-k^2]}\left(1-\frac{k^2}{p^2+(k-p)^2}\right)\right]-\frac{1}{2\mu p^2}\left(1-\frac{k^2}{p^2}\right)\mathbf{k}\cdot(\mathbf{k}-\mathbf{p}), \quad (61)$$

$$\tilde{D}_{uu}=D_{uu}+\Delta\frac{D^2_{uu}}{\nu^2k^{1-s}}, \quad (62)$$

$$\tilde{D}_{bb}=D_{bb}+\Delta\frac{D^2_{bb}}{\nu^2k^{1-s}}, \quad (63)$$

$$\tilde{D}_{ub}=D_{ub}, \quad (64)$$

where Δ is just a numerical constant. The self-consistent solution is given by $\nu,\mu\sim k^{(1-s)/2}$, with the long-wavelength behaviors of D_{uu}, D_{bb}, and D_{ub} unchanged. Now we can easily calculate the decay of the total velocity and magnetic energy, and cross helicity; these are

$$E^v(t)\sim t^{-(6-2s)/(2-s)}, \quad (65)$$

$$E^b(t)\sim t^{-(6-2s)/(2-s)}, \quad (66)$$

and

$$H^c(t)\sim t^{-(6-2y)/(2-s)}. \quad (67)$$

Here $E^v=\int d^dk\,1/2\langle|v(k)^2\rangle$, $E^b=\int d^dk\,1/2\langle|b(k)^2\rangle$, $H^c=\int d^dk|\mathbf{v}(\mathbf{k})\cdot\mathbf{b}(\mathbf{k})|$ are total velocity-field and magnetic-field energies, and total cross helicity, respectively. While calculating the temporal decay of these quantities it has been implicitly assumed that the lower and the upper limits of the momentum integrals can be extended up to 0 and ∞, respectively; if this not possible temporal behavior cannot be obtained by scaling (see next section).

Decay of fully developed MHD turbulence

In fully developed 3D MHD turbulence one finds, in the inertial range,

$$\langle v_i(\mathbf{k},t)v_j(\mathbf{k}',t)\rangle\sim P_{ij}(\mathbf{k})k^{-11/3}\delta(\mathbf{k}+\mathbf{k}'), \quad (68)$$

$$\langle b_i(\mathbf{k},t)b_j(\mathbf{k}',t)\rangle\sim P_{ij}(\mathbf{k})k^{-11/3}\delta(\mathbf{k}+\mathbf{k}'). \quad (69)$$

Of course, a study of higher-order correlation functions reveals that the velocity and magnetic-field distributions are not Gaussian [7]. If, however, for the purpose of analytical tractability, we assume that the initial distributions are Gaussian with the variances as (for our Burges-type model)

$$\langle u_i(\mathbf{k},t=0)u_j(\mathbf{k}',t=0)\rangle = D_{uu}k_ik_j|k|^{-11/3-2}, \quad (70)$$

$$\langle b_i(\mathbf{k},t=0)b_j(\mathbf{k}',t=0)\rangle = D_{bb}k_ik_j|k|^{-11/3-2}, \quad (71)$$

such that $|\langle u(k,t=0)u(-k,t=0)\rangle| \sim |\langle b(k,t=0)b(-k,t=0)\rangle| \sim k^{-11/3}$ as observed in fully developed MHD turbulence, we can calculate z and effective two-point correlations as we did above in Sec. III A. For simplicity, we give details only for our simple Burgers-type model [Eqs. (3), (4)]. The effective ν, D_{uu}, and D_{bb} are given by

$$\frac{1}{\tilde{\nu}k^2} = \frac{1}{\nu k^2} + \frac{D_{uu}}{\nu k^2}\int d^d p \, \frac{p_l p_m p^{-11/3-2} k\cdot(\mathbf{k}-\mathbf{p})}{2\nu \mathbf{k}\cdot\mathbf{p}}\left[\frac{1}{2\nu p^2 - 2\nu \mathbf{k}\cdot\mathbf{p}}\left(1-\frac{k^2}{\nu[p^2+(\mathbf{k}-\mathbf{p})^2]}\right) - \frac{1}{2\nu p^2}\left(1-\frac{k^2}{2\nu p^2}\right)\right]$$
$$+ \frac{D_{bb}}{\nu k^2}\int d^d p \, \frac{p_l p_m p^{-11/3-2} \mathbf{k}\cdot(\mathbf{k}-\mathbf{p})}{2\mu \mathbf{k}\cdot\mathbf{p}}\left[\frac{1}{2\mu p^2}\left(1-\frac{\nu k^2}{2\mu p^2}\right) - \frac{1}{2\mu p^2}\left(1-\frac{\nu k^2}{2\mu p^2}\right)\right], \tag{72}$$

$$\tilde{D}_{uu} = D_{uu} + \delta\frac{D_{uu}^2}{\nu^2 k^{8/3}} + \delta\frac{D_{bb}^2}{\mu^2 k^{8/3}}, \tag{73}$$

$$\tilde{D}_{bb} = D_{bb} + 2\delta\frac{D_{bb}D_{uu}}{\mu^2 k^{8/3}}. \tag{74}$$

Here δ is a numerical constant. The self-consistent solutions of these equations are given by $\nu, \mu \sim k^{-4/3}$ and $\tilde{D}_{uu} = \tilde{D}_{bb}$, implying that $z = 2/3$; this is the same as in the steady state. With this self-consistent solution, we see that the one-loop corrections to D_{uu} and D_{bb} are as singular as the bare quantities. Hence we ignore their renormalizations. When D_{ub} is nonzero, it will contribute to the one-loop corrections of D_{uu} and D_{bb} with the same low-wave-number singularity. D_{ub} itself does not have any diagrammatic correction, as in the case discussed in Sec. III.

The decay of two-point correlation functions will be of the form

$$\langle u_i(\mathbf{x},t)^2\rangle \sim \int d^3k \exp(-2\nu k^{2/3} t) k^{-11/3}. \tag{75}$$

It is easy to see that, because of the infrared divergence of the integral, the lower limit cannot be extended to 0, so it will depend upon a lower cutoff (the inverse of which is the integral scale). Consequently the t dependence cannot be scaled out as in the previous case. This problem is reminiscent of the sweeping divergence that appears in a perturbative DRG calculation of fully developed turbulence or MHD turbulence [9,12]. In fact this problem begins when $\langle u_i(\mathbf{k},0)u_j(\mathbf{k}',0)\rangle \sim k^{2-2y/3-d}$ and $y=3$; then the above integral becomes log divergent. This type of initial state can be prepared by randomly stirring the system with a stochastic force with a variance k^{4-y-d} with $y=3$. In a DRG analysis, sweeping divergences appear when $y \geq 3$ (but $K41$ scaling obtains for $y=4$) [12]. Higher-order correlation functions have more severe divergences, hence their decay also depend strongly upon the integral scale.

V. CONCLUDING REMARKS

We have examined the decay of the total kinetic and magnetic energies, and the cross helicity in our shell model, These quantities decay with power laws in time. In order to understand this behavior analytically, we have employed a one-loop perturbation theory. In the first part of our calculations, we have chosen random initial conditions with the statistical properties given in Eqs. (5), (6) and (10), (11) (with no cross correlations). We have shown that such initial conditions lead to a power-law decay of temporal correlations and appropriately defined structure functions. For initial correlations analytic in the long-wavelength limit no higher-order structure functions show any anomalous scaling. However, on introducing cross correlations $\langle u_i(\mathbf{k},0)b_j(\mathbf{k}',0)\rangle$ [Eq. (43)] higher-order structure functions exhibit anomalous scaling. This highlights the importance of cross corrreations in the statistical properties of MHD turbulence. We have also extended our calculations to the case of initial correlations with singular variances and discussed the difficulties in the decay of fully developed MHD turbulence. We have argued that these difficulties are related to the sweeping effect which arises in the study of the stochastically driven MHD turbulence (in the statistically steady state). It is also worth noting that we have obtained similar temporal behavior from both 3D MHD and our simplified Burgers-type model. It would be interesting to see if our results can be checked experimentally and numerically.

ACKNOWLEDGMENTS

The author thanks Rahul Pandit, Sriram Ramaswamy, and Jayanta K. Bhattacharjee for discussions. The author acknowledges CSIR (India) for financial support.

[1] M. R. Smith, R. J. Donnelly, N. Goldenfeld, and W. F. Vinen, Phys. Rev. Lett. **71**, 2583 (1993).
[2] G. Comte-Bellot and S. Corrsin, J. Fluid Mech. **25**, 657 (1966).
[3] M. M. Low, R. S. Klessen, and A. Burkert, astro-ph/9712013.
[4] M. Hossain, P. C. Gray, D. H. Pontius, Jr., and W. H. Matthaeus, Phys. Fluids **7**, 2886 (1995).
[5] S. Galtier, H. Politano, and A. Pouquet, Phys. Rev. Lett. **79**, 2807 (1997).
[6] D. Biskamp and W. Müller, Phys. Rev. Lett. **83**, 2195 (1999).
[7] A. Basu, A. Sain, S. K. Dhar, and R. Pandit, Phys. Rev. Lett. **81**, 2685 (1998).

[8] V. Periwal, Phys. Lett. A **231**, 235 (1997).
[9] A. Basu, J. K. Bhattacharjee, and S. Ramaswamy, Eur. Phys. J. B **9**, 725 (1999).
[10] D. Forster, D. R. Nelson, and M. J. Stephen, Phys. Rev. A **16**, 732 (1977).
[11] V. Yakhot and S. A. Orzag, J. Sci. Comput. **1**, (1986).
[12] C.-Y. Mou and P. B. Weichman, Phys. Rev. E **52**, 3738 (1995).